REFERENCES

[1] M. W. Pospieszalski, "Modeling of noise parameters of MESFET's and their frequency and temperature dependence," *IEEE Trans. Microwave Theory Tech.*, vol. 37, no. 9, Sept. 1989, pp. 1340–1350.

[2] P. J. Tasker, W. Reinert, B. Hughes, J. Braunstein, and M. Schlechtweg, "Transistor noise parameter extraction using 50 ohm measurement system," in 1993 *MTT-S Int. Microwave Symp. Dig.*, pp. 1251–1254.

[3] G. Martines and M. Sannino, "A method for measurement of losses in the noise-matching microwave network while measuring transistor noise parameters," *IEEE Trans. Microwave Theory Tech.*, vol. MTT-35, no. 1, pp. 71–75, Jan. 1987.

[4] A. Davidson, B. Leake, and E. Strid, "Accuracy factors in microwave noise parameter measurements," in *1989 MTT-S Int Microwave Symp. Dig.*, pp. 827–830.

[5] L. Escotte, R. Plana, and J. Graffeuil, "Evaluation of Noise Parameter Extraction Methods," *IEEE Trans. Microwave Theory Tech.*, vol. 41, no. 3, Mar. 1993.

[6] E. Strid, "Noise measurements for low-noise GaAs FET amplifiers," *Measurements Techniques*, pp. 62–70, Nov. 1981.

[7] G. F. Engen and C. A. Hoer, "Thru-reflect-line: An improved technique for calibrating the dual six-port automatique network analyzer," *IEEE Trans. Microwave Theory Tech.*, vol. 27, no. 12, pp. 987–993, Dec. 1979.

[8] R. Pantoja *et al.*, "Improved calibration and measurement of the scattering parameters of microwave integrated circuits," *IEEE Trans. Microwave Theory Tech.*, vol. 37, no. 11 , pp. 1675–1680, Nov. 1989.

[9] G. Vasilescu, G. Alquie, and M. Krim, "Exact computation of two-port noise parameters," *Electron. Lett.*, vol. 25, no. 4, Feb. 16, 1989.

[10] NEC Data Book, "RF and Microwave Semiconductors," Ca. Eastern Lab., pp. 1–94, 1994.

[11] NEC Microwave Semiconductor Devices, "Design Parameter Library, Vers. 6," Ca. Eastern Lab.

The Analysis of General Two-Dimensional PEC Structures Using a Modified CPFDTD Algorithm

Chris J. Railton, Ian J. Craddock, and John B. Schneider

Abstract—**The use of the contour path finite difference time domain (CPFDTD) method with locally distorted contours has been shown to give accurate results for curved metal structures. However, the numerical stability of this scheme is not guaranteed and significant skill is required in order to generate an appropriate grid. In this contribution, we present a modification to the CPFDTD scheme which ensures stability and give a step-by-step procedure for simple generation of the distorted grid. Examples are presented to demonstrate that the modified scheme yields results superior to those obtained using the standard staircased finite difference time domain (FDTD) approach. Example geometries are cylindrical cavities having complex cross-sections with smooth surfaces and right-angle bends. The accuracy of the method is demonstrated by comparison to analytical results where available.**

I. INTRODUCTION

The electromagnetic analysis of complex, curved metal structures using the finite difference time domain (FDTD) technique has proved a difficult challenge and one which has not yet been satisfactorily resolved. Such problems do, however, occur in a wide variety of application areas ranging from propagation in waveguides to scattering from aircraft fuselages. Attempts to overcome the difficulties associated with this type of problem include the use of globally distorted meshes [1]–[3] and the incorporation of static field solutions (SFS) into the standard Cartesian mesh [4], [5]. The former requires approximately three times the computer resources of the standard Cartesian FDTD at the same number of points per wavelength [2], while the latter, in its present state of development, is prone to late-time instability.

A third approach to the problem is to use a locally distorted mesh where the basic Cartesian grid is modified only in the vicinity of the metal boundaries. One such scheme, the contour path finite difference time domain (CPFDTD) scheme, is formulated in terms of the integral form of Maxwell's equations instead of the usual differential form [6], [7]. A major advantage of this approach when compared to other conformal techniques is that the simplicity and efficiency of the Cartesian mesh is retained throughout the majority of the problem space and only those nodes which are adjacent to the curved surface need be given special attention. In addition, the algorithms for absorbing boundaries, near-to-far field transformations and Huygens' sources, which are well developed for the standard FDTD method, can be applied without change.

Despite the fact that this type of algorithm appears to allow the efficient analysis of very complex structures, comparatively little use of the method has been reported. Some researchers have called into question the stability of the original CPFDTD scheme since it employs a noncausal and nonreciprocal "nearest neighbor" approximation [3], [8], [9]. Despite the fact that stability cannot be guaranteed, it appears that, with appropriate grid selection, instabilities may be weak enough so as not to preclude using the original CPFDTD scheme for particular open-domain problems [9]. For lossless resonant structures, however, for which there is no mechanism for dissipating spuriously generated energy, meaningful results are not usually obtainable [9], [10].

In this contribution we present a modified form of the two-dimensional (2-D) CPFDTD algorithm which overcomes these problems without sacrificing accuracy. This modification recasts the "nearest neighbor" approximation, employed in standard CPFDTD, such that reciprocal interaction of nodes is obtained. Examination of the update equations for those E field nodes whose values are borrowed by neighboring cells and for the H field cells which are directly affected by them, shows that the original CPFDTD spatial discretization scheme is likely to produce a system which does not comply with the law of conservation of energy. It can also be shown that grids which allow extended contours to overlap may not conserve energy. Since, in these cases, the instability is inherent in the *spatial* discretization, there will exist no choice of time step which will yield a stable solution. Before it is useful to consider the problem of determining the CFL limit for the modified *difference* scheme, it is necessary to ensure that the underlying *differential* scheme is energy conserving. The modification described in this contribution yields a system whose update equations are identical to those of a passive electrical network consisting only of capacitors and gyrators which must necessarily conserve energy [11].

In this paper the nature of the instabilities which can occur in the standard CPFDTD algorithm is discussed, then, a step-by-step procedure is presented whereby the energy conserving CPFDTD mesh can be generated. Finally the use of the method is demonstrated

Manuscript received August 22, 1995; revised June 14, 1996.

C. J. Railton and I. J. Craddock are with the Centre for Communications Research, Faculty of Engineering, University of Bristol, Bristol, BS8 1TR, UK.

J. B. Schneider is with the School of Electrical Engineering and Computer Science, Washington State University, Pullman, WA 99164-2752 USA.

Publisher Item Identifier S 0018-9480(96)06910-4.

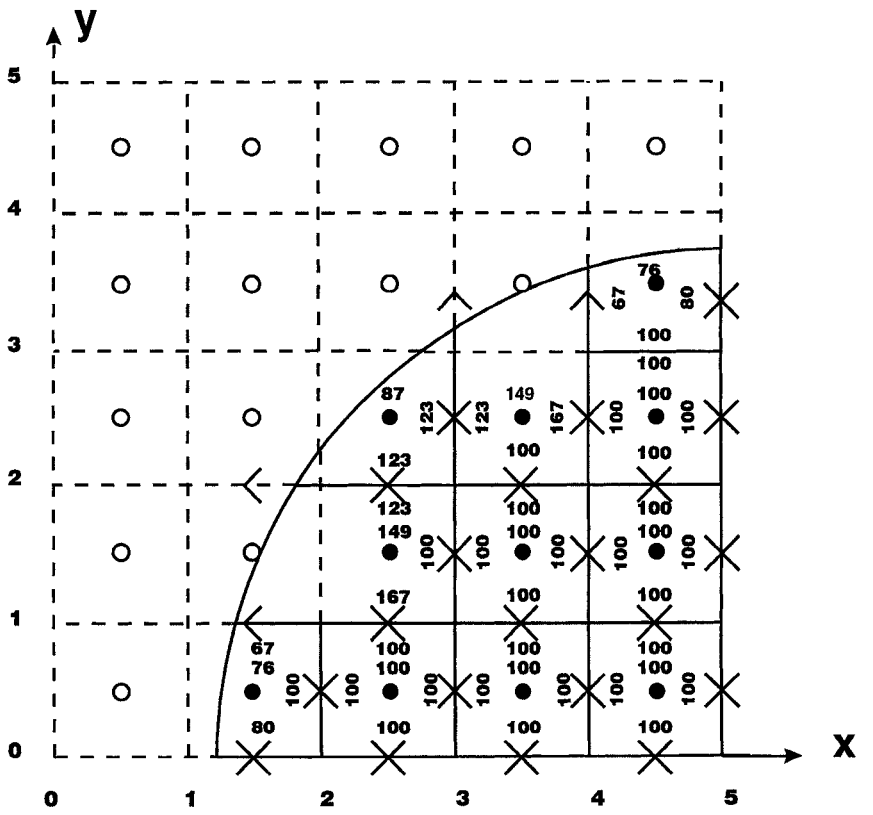

Fig. 1. The CPFDTD method applied to a cylinder.

for the analysis of a square resonator, rotated with respect to the grid, and of a resonator with complex cross-section. By comparison to analytical results for the square resonator the accuracy of the scheme is shown. The accuracy and convergence properties are further demonstrated, using the complex resonator, by varying the unit cell size over a broad range. For the geometries presented here, and for all other geometries to which the algorithm has been applied, numerical stability was **always** achieved without reducing the time step below that used for the standard FDTD scheme.

An alternative scheme aimed at solving similar problems to those addressed in this paper was presented in [12] and further developed in a very recent publication, [13]. Although the algorithm described here is based on a generalization of the CPFDTD scheme whereas that in [13] is based on a generalization of the TLM method, the two algorithms have some aspects in common. The relative accuracy and efficiency of these two schemes remains an open question.

II. The Nature of the Instability

As explained in [10], the root of the instability problem in the standard CPFDTD approach can be traced to those E nodes whose values are borrowed from neighboring distorted cells. Consider the cross-section of a circular cylindrical resonator, a quarter of which is shown in Fig. 1. Here, the grid for the TE problem is shown where the H_z nodes are indicated by circles and are located at the centre of each undistorted cell. The E_x and E_y nodes are marked by crosses or arrows and are found along the edges of cells. The magnetic field is assumed to be constant over the area of a given cell while electric fields are assumed to be constant over the length of the edge corresponding to a given node. Dashed lines indicate edges which are not used in the scheme. The E nodes represented by arrows cannot be calculated directly using the FDTD scheme because one or both of the H_z nodes required in the corresponding update equation is in the metal. Following [6] these nodes borrow their value from the nearest available collinear E field component. The numbers in the centre of each square are the areas enclosed by the Faraday contours and the numbers next to the edges are the lengths of the straight sections of the associated contour. In each case the values are normalized so that values of 100 correspond to an unmodified cell. Although the grid shown in Fig. 1 appears to be the most obvious way of implementing the CPFDTD algorithm, it is not difficult to demonstrate that such an implementation leads to numerical instability. We may show this by considering the scheme in matrix form thus

$$\frac{\partial^2 \underline{\underline{E}}}{\partial t^2} = \underline{\underline{A}}\,\underline{\underline{B}}\,\underline{\underline{E}} \tag{1}$$

where $\underline{\underline{E}}$ is the vector formed by the values of all the E field nodes in the mesh, and $\underline{\underline{A}}$ and $\underline{\underline{B}}$ are matrices containing the coefficients of the update equations for the E and H nodes, respectively. The elements of these two matrices differ from the coefficients of the usual CPFDTD update equations only insofar as there is no factor δt, i.e., at this point the system is assumed to be a continuous time system. Equation (1) has the solution

$$\underline{\underline{E}} = \sum_i \underline{\underline{k}}_i e^{(\sigma_i + j\omega_i)t} \tag{2}$$

where $\underline{\underline{k}}_i$ is the ith eigenvector of the matrix $\underline{\underline{AB}}$ and $(\sigma_i + j\omega_i)^2$ is the corresponding eigenvalue. The condition for stability is that none of the values of σ_i be greater than zero. If the discretised scheme correctly represents a lossless situation then σ_i would be zero for all values of i. This is not the case for the nearest-

TABLE I
PARAMETERS USED IN THE GENERATION OF THE MODIFIED CPFDTD MESH

Name	Associated Quantity	Default Value	Comment
inside_metal	H_z	*false*	*true* if H_z is inside metal
ex_available	E_x	*true*	*false* if either of the neighbouring H_z nodes are in metal
ey_available	E_y	*true*	*false* if either of the neighbouring H_z nodes are in metal
ex_exist	E_x	*true*	*false* if edge is not used in the CPFDTD algorithm
ey_exist	E_y	*true*	*false* if edge is not used in the CPFDTD algorithm
ex_from	E_x	0	Integer offset used to point to borrowed E_x nodes
ey_from	E_y	0	Integer offset used to point to borrowed E_y nodes

neighbor discretization associated with Fig. 1. It is emphasised that since only the *spatial* discretization is being examined here, this instability will exist regardless of the time step used, i.e., the system is *unconditionally unstable.*

Referring to Fig. 1, the update equation for H_z (1.5, 0.5) is given by

$$H_z^{n+1}(1.5,0.5) = H_z^n(1.5,0.5) + \frac{\delta t}{\mu\delta}\left(\frac{100}{76}E_y^{n+1/2}(2,0.5) + \frac{80}{76}E_x^{n+1/2}(1.5,0) - \frac{67}{76}E_x^{n+1/2}(2.5,1)\right) \tag{3}$$

where $E_x(2.5,1)$ is the borrowed node, δt is the time step and δ is the space step.

The update equation for $E_x(2.5,1)$ is given by

$$E_x^{n+1/2)}(2.5,1) = E_x^{n-1/2}(2.5,1) + \frac{\delta t}{\epsilon\delta}(H_z^n(2.5,1.5) - H_z^n(2.5,0.5)). \tag{4}$$

It can be seen that no corresponding inclusion of $H_z(1.5,0.5)$ exists. This scheme represents an unphysical situation which, therefore, cannot be guaranteed to behave in an energy conserving manner.

In order to remedy the situation, we must modify this equation to include the missing term. This can be done as follows:

$$E_x^{n+1/2}(2.5,1) = E_x^{n-1/2}(2.5,1) + \frac{\delta t}{\epsilon\delta} \cdot \left(H_z^n(2.5,1.5) - \frac{67}{167}H_z^n(1.5,0.5) - \frac{100}{167}H_z^n(2.5,0.5)\right). \tag{5}$$

Here we have taken a weighted average of the two H_z nodes which have a dependence on $E_x(2.5,1)$ through the contour segment with a total length of 167, with the weights being in the same ratio as the strengths of the corresponding dependencies. In general, the modified update equations use a weighted average of the H_z nodes to ensure that the nodes associated with a borrowed value interact reciprocally. As well as being intuitively more reasonable, this change makes it possible to prove that the resulting scheme is the analogue of a passive circuit consisting entirely of capacitors and gyrators [11]. The system must, therefore, conserve energy. Calculation of the eigenvalues of the new scheme confirms that, indeed, all values of σ_i are zero.

III. A PROCEDURE FOR GENERATING THE CPFDTD GRID

To facilitate the generation of the modified CPFDTD grid for arbitrary metal objects we first define some parameters. These are summarized in the Table I.

With each H node a flag is associated which indicates whether or not that node is inside the metal. With each E node two flags are associated. One flag indicates whether it can be updated using H nodes which are outside the metal and is therefore *available* from the standpoint of the standard FDTD equations. The other flag indicates whether any portion of the edge associated with a node will be used in the final mesh and will therefore *exist*. Ultimately, the status of some nodes will be that they *exist* but are not *available*. For these nodes it is then necessary to borrow values from neighboring nodes. Therefore, for each E node an integer offset, *from*, is used to indicate from where its value must be borrowed (a value of zero indicates that no borrowing is necessary).

To generate the mesh and the associated update equations, we use the following procedure:

1) For each H node, set the *inside_metal* flag to *true* if the node is inside the metal.
2) For each E node in the mesh set the flag *available* to *false* if either of the H nodes whose values are required in the standard FDTD update equation are inside the metal.
3) For each E node set the *exist* flag to *false* if the corresponding edge is totally inside the metal.
4) For each H node which is inside the metal and whose surrounding undistorted contour intersects the metal boundary, set the *exist* flag of one and only one of the surrounding E nodes to *false* so as to join the contour to that of the neighboring node which has the largest number of available surrounding E nodes.
5) For each E node which is not *available* but does *exist* set the *from* offset to the nearest collinear node which is *available.*
6) For each H node, which is not inside the metal, calculate the lengths of each straight section of the distorted Faraday contour. Additionally, calculate the area of the surface surrounded by the contour.

TABLE II
PERCENTAGE ERROR IN THE RESULTS FOR A ROTATED SQUARE RESONATOR OF SIDE 30 cm AND UNIT CELL SIZE δ

	Staircase Approximation				Modified CFDTD			
	Mode 1		Mode 3		Mode 1		Mode 3	
Angle	δ=5cm	δ=2.5cm	δ=5cm	δ=2.5cm	δ=5cm	δ=2.5cm	δ=5cm	δ=2.5cm
0°	-0.72	-0.26	-2.85	-0.77	-0.72	-0.26	-2.85	-0.77
5°	-0.72	-0.26	-2.85	-0.77	-0.60	-0.14	-2.42	-0.45
10°	-0.72	-2.66	-2.85	-6.91	-0.10	-0.02	-0.93	-0.53
15°	-6.44	-1.46	13.3	-1.53	0.12	0.04	-1.41	-0.29
20°	-6.44	-3.90	13.3	-0.92	0.40	0.36	-0.39	-0.21
25°	-12.38	-3.80	13.6	-5.06	0.90	0.90	-1.25	0.30
30°	-4.44	-4.76	13.6	-0.81	0.08	1.08	0.14	0.70
35°	-4.44	-3.60	13.6	-6.04	1.42	1.18	1.20	0.80
40°	-4.44	-3.10	12.2	-4.33	3.36	1.34	2.20	0.70
45°	-10.42	-3.06	-8.12	-3.54	1.86	1.78	0.10	1.00

7) Referring to (3), for each H node which is not inside the metal we set the numerators and denominators of each fraction multiplying the E field nodes as follows. Set all the denominators equal to the area surrounded by the Faraday contour. Set each numerators equal to the length of that part of the Faraday contour which passes through the E node with which it is associated.
8) Referring to (5), for each E node which is available we set the numerators and denominators of each fraction multiplying the H field nodes as follows: Set all denominators equal to the length of the edge containing the E node. Set each numerator equal to the length of that part of the edge which coincides with the Faraday contour of the associated H node.

As an example we use the cylinder shown in Fig. 1:

1) The H_z nodes at [0, 0], [0, 1], [0, 2], [0, 3], [0, 4], [1, 1], [1, 2], [1, 3], [1, 4], [2, 3], [2, 4], [3, 3], [3, 4], [4, 4] are *inside_metal.*
2) The nodes $E_x[1,1]$, $E_x[2,3]$, $E_x[3,3]$, $E_x[4,4]$ and $E_y[1,0]$, $E_y[2,1]$, $E_y[2,2]$, $E_y[4,3]$ are not *available.*
3) The flags *ex_exist* at [0, 0], [0, 1], [0, 2], [0, 3], [0, 4], [1, 3], [1, 4], [2, 4], [3, 4], [4, 4] are set to *false.* The flags *ey_exist* at [0, 0], [0, 1], [0, 2], [0, 3], [0, 4], [1, 0], [1, 1], [1, 2], [1, 3], [1, 4], [2, 3], [2, 4], [3, 4], [4, 4] are set to *false.*
4) The flags *ey_exist* at [2, 1], [2, 2] and the flags *ex_exist* at [2, 3], [3, 3] are set to *false.*
5) The offsets are set as: *ex_from* [1, 1] = 1, *ey_from* [3, 3] = −1, *ex_from* [1, 2] = 1, *ey_from* [4,3] = −1 all others to zero.
6) The values of the areas and the lengths of edges are calculated as shown on Fig. 1.
7) The denominators of the fractions in the H field update equations are just those shown on Fig. 1 as areas. The numerators are given by the lengths, also shown on Fig. 1.
8) The numerators and denominators of the fractions in the E field update equations are given by the lengths shown on Fig. 1.

IV. THE CHOICE OF TIME STEP

Having established that the spatial discretization scheme is energy conserving, it is now appropriate to consider the maximum time step which is allowed. The CFL limit for the standard FDTD scheme can be established by the following condition. The time step must be small enough so that the domain of dependence of the time discretised scheme is greater than, or equal to, that of the underlying differential equations. For the FDTD scheme the time step limit can be found by considering propagation in the diagonal direction. Maxwell's equations dictate that free space propagation between neighboring diagonal nodes requires a time of $\sqrt{2\delta/c}$. In the time discretised scheme this requires 2 time steps. This leads to the well known condition: $\delta t < \delta/(c\sqrt{2})$ for stability. Consideration of the modified CPFDTD scheme shows that no worse case than this has been introduced and therefore the CFL condition is unaltered.

V. NUMERICAL RESULTS

In order to demonstrate both the stability and accuracy of the scheme, the resonant frequencies of the TE modes of a rotated square cylinder and of a cylinder with a complex cross-section have been calculated. (The TM cases require no modification to the standard CPFDTD scheme since, in this case, the scheme can be shown to be physically realizable as no borrowing from neighboring distorted cells is necessary.) Results for the case of a circular cylinder have previously been presented in [10]. All these results were obtained using 8000 time steps. Additional runs were done using 32 000 time steps and no instability was ever observed.

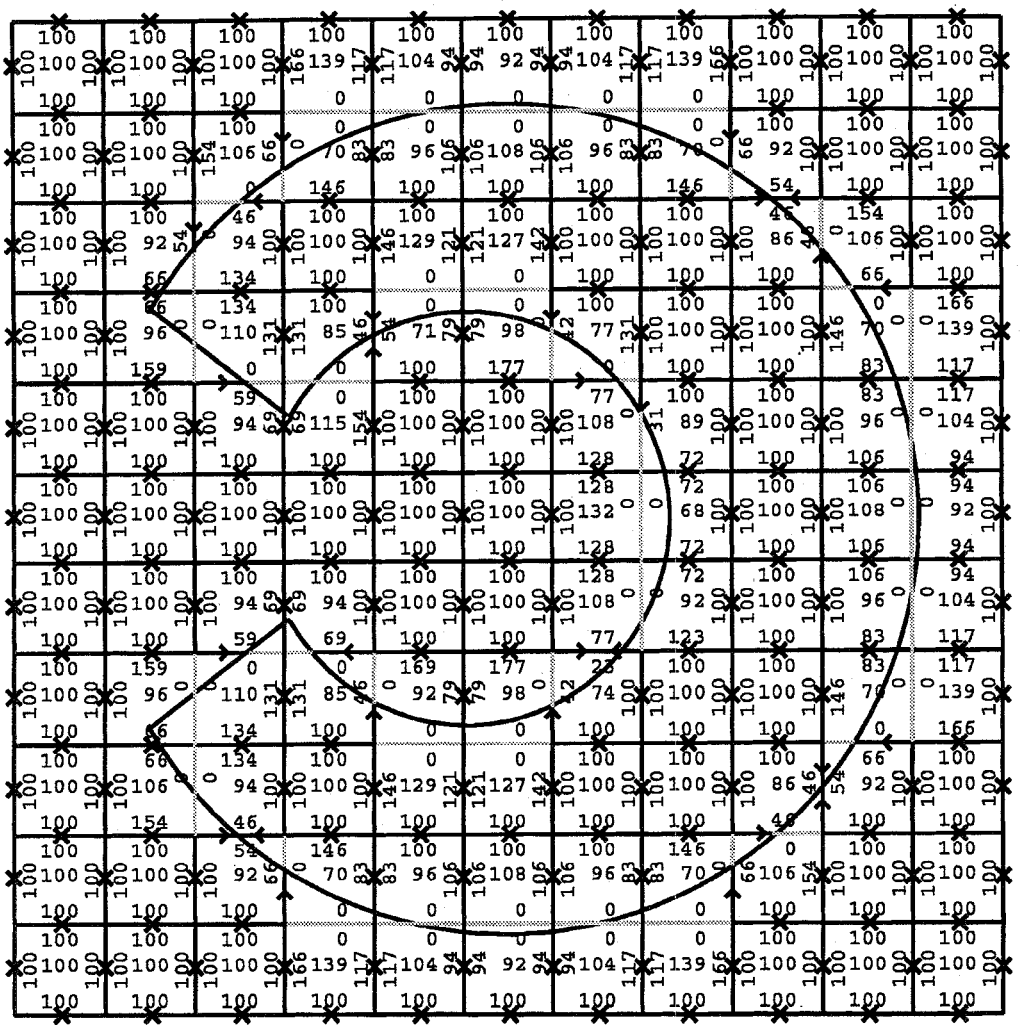

Fig. 2. The distorted grid used for the "keyhole" waveguide.

TABLE III
RESULTS FOR THE RESONANT FREQUENCIES OF A KEYHOLE RESONATOR VERSUS CELL SIZE δ

	Staircase Approximation				Modified CPFDTD			
	δ=24cm	δ=12cm	δ=4cm	δ=3cm	δ=24cm	δ=12cm	δ=4cm	δ=3cm
Mode 1	68.4	77.3	76.6	77.0	80.4	79.9	79.2	79.1
Mode 2	104.1	110.8	114.8	115.1	117.5	116.8	116.0	115.3
Mode 3	133.1	147.8	148.9	150.5	155.9	115.7	154.3	154.0
Mode 4	166.6	178.0	184.0	185.7	191.4	191.4	190.3	188.4

A. Rotated Square Cylinder

The error in the calculated resonant frequencies of the first and third modes of a rotated square resonator for the staircase approximation and for the method described in this paper are shown in Table II. It can be seen that the error from the modified CPFDTD technique is consistantly less than with the staircase method.

B. Keyhole Waveguide

As an example of a more complex structure, the "keyhole" waveguide, similar to that treated by Das *et al.* [14], who used a conformal mapping technique, was analyzed. The first four resonant modes of this structure were calculated using a range of cell sizes in order to establish the convergence properties of the modified technique when compared to the staircase approach. The geometry of this structure and an example of the deformed grid used is given in Fig. 2. In this case a grid has been generated which is valid for the interior and the exterior problem. The calculated resonant frequencies versus cell size is shown in Table III together with the results of the staircased FDTD. It can be seen that consistent results are obtained from the modified CPFDTD scheme even with a very coarse mesh, whereas

the discrepancy using the staircase approximation increases rapidly as the cell size is increased.

VI. Conclusion

A simple and effective modification to the well known locally distorted CPFDTD algorithm has been described and a step-by-step procedure for the simple generation of the modified grid has been presented. The fact that the modified scheme is formally equivalent to a passive electrical circuit consisting of capacitors and gyrators ensures that it does not suffer from the instability inherent in the nearest-neighbor approximation. The robustness, stability and accuracy of the scheme has been verified for cylindrical resonators of complex cross-section, including right-angled corners. Trials have also been performed with many other structures such as parallel-plate-waveguide containing S bends. In all cases the algorithm remained stable and accurate. It is anticipated that the added robustness which the modification provides will facilitate more widespread use of the CPFDTD algorithm. Furthermore, building on the techniques described here, it is possible to develop a stabilised CPFDTD scheme applicable to three-dimensional (3-D) problems. This extension is the subject of ongoing work and will be described in a future contribution.

Acknowledgment

The authors at the University of Bristol wish to thank Prof. J. McGeehan for the provision of facilities at the Centre for Communications Research.

References

[1] R. Holland, "Finite difference solutions of Maxwell's equations in generalized nonorthogonal coordinates," *IEEE Trans. Nucl. Sci.*, vol. NS-30, no. 6, 1983, pp. 4589–4591.

[2] J.-F. Lee, and R. Palandech, and R. Mittra, "Modeling three-dimensional discontinuities in waveguides using non-orthogonal FDTD algorithm," *IEEE Trans. Microwave Theory Tech.*, vol. 40, Feb. 1992, pp. 346–352.

[3] N. K. Madsen, "Divergence preserving discrete surface integral methods for Maxwell's curl equations using non-orthogonal unstructured grids," Rep. UCRL-JC-109787, Lawrence Livermore National Lab., 1992.

[4] D. B. Shorthouse and C. J. Railton, "The incorporation of static field solutions into the finite difference time domain algorithm, *IEEE Trans. Microwave Theory Tech.*, vol. 40, May 1992, pp. 986–994.

[5] C. J. Railton, "Use of static field solutions in the FDTD method for the efficient treatment of curved metal surfaces," *Electronics Lett.*, Aug. 1993, pp. 1466–1467.

[6] T. G. Jurgens, A. Taflove, K. Umashankar and T. G. Moore, "Finite-Difference Time-Domain Modeling of Curved Surfaces," *IEEE Trans. Antennas Propagat.*, vol. 40, Apr. 1992, pp. 357–366.

[7] T. G. Jurgens and A. Taflove "Three-dimensional contour FDTD modeling of scattering from single and multiple bodies," *IEEE Trans. Antennas Propagat.*, vol. 41, Dec. 1993, pp. 1703–1708.

[8] M. Okoniewski, J. Anderson, M. Mrozowski, and S. S. Stuchly, "Arbitrarily located metal surfaces in FDTD technique," Progress in Electromagnetics Res. Symp., pp. 178, Seattle, WA, July 1995.

[9] J. Anderson, M. Okoniewski and S. S. Stuchly, "3-D FDTD treatment of perfect electric conductors," in *Dig. URSI Meet.* Newport Beach, CA, 1995, p. 257.

[10] C. J. Railton, I. J. Craddock, and J. B. Schneider, "Improved locally distorted CPFDTD algorithm with provable stability," *Electronics Lett.*, vol. 31, no. 18, 31 Aug. 1995, pp. 1585, 1586.

[11] I. Craddock and C. J. Railton, "Derivation and application of a passive equivalent circuit for the FDTD algorithm." *IEEE Microwave Guided Wave Lett.*, Jan. 1996.

[12] W. K. Gwarek, "Analysis of arbitrarily-shaped planar circuits—a time domain approach" IEEE Trans MTT-33, pp 1067–1072, Oct. 1985.

[13] M. Celuch-Marcysiak and W. K. Gwarek, "Generalized TLM algorithms with controlled stability margin and their equivalence with finite difference formulations for modified grids," *IEEE Trans. Microwave Theory Tech.*, vol. 43, pp. 2081–2089, Sept. 1995.

[14] B. N. Das, S. B. Chakrabarty, and A. K. Mallick, "Cutoff frequencies of guiding structures with circular and planar boundaries," *Microwave and Guided Wave Lett.*, vol. 5, no. 6, June 1995, pp. 186–188.

CAD Model for Coplanar Waveguide Synthesis

Tianquan Deng

***Abstract*—Accurate closed-form synthesis formulas for coplanar waveguides are presented for CAD applications, which are approximated in terms of ordinary functions. These formulas are derived, based on function approximation and curve-fitting correction of quasi-static numerical results. Comprehensive comparisons have been made by using results from the quasi-static analysis, the rigorous full-wave analysis, and the experiment available in the literature. Accuracy is found to be better than 1.5 percent for the practical range. The application range of frequency is within the limits well known for quasi-static TEM approximation and can be applied up to 20 GHz.**

I. Introduction

Recent progress in monolithic microwave integrated circuits (MMIC) and millimeter-wave integrated circuits (MMWIC) has initiated an extensive study of coplanar waveguides (CPW) due to several advantages offered over conventional microstrip lines [1], [2]. These advantages include ease of parallel and series insertion of both active and passive components and high circuit density. Another feature of coplanar waveguide is that its traces can be changed to match component lead widths while keeping the characteristic impedance constant. Most of the study efforts have been directed towards the obtaining of design parameters by either full-wave numerical methods [3]–[6] or quasi-static conformal mapping methods [7]–[12]. Full-wave analyses provide high precision in a wide frequency band. On the other hand quasi-static methods lead to closed-form expressions suitable for CAD software packages and they provide a simulation accuracy comparable with full-wave methods for frequencies up to 20 GHz [1], [13]. More recently CAD models for coplanar waveguides have received considerable attention [13]–[15]. It is noted that so far, all of the conventional CAD models for coplanar waveguides are analysis models that are used to obtain electrical parameters by the use of geometrical parameters of CPW structures. No closed-form synthesis formulas for coplanar waveguides are available; in contrast, both analysis and synthesis closed-form formulas for microstrip lines have existed for a long time [16], [17]. Such closed-form synthesis formulas provide a convenient way for designers to directly obtain the physical dimensions of CPW structures for the required design specifications rather than through an iteration approach using the conventional design equations. They

Manuscript received September 14, 1995; revised June 14, 1996.

The author was with the Institute of Microwave Electronics, University of Electronic Science and Technology of China, PRC. He is now with the Department of Electrical Engineering, National University of Singapore, Singapore.

Publisher Item Identifier S 0018-9480(96)06911-6.